

# Biocalcification in porcelaneous foraminifera

Reviewed Preprint

v2 • July 9, 2024

Revised by authors

Reviewed Preprint

v1 • February 2, 2024

Zofia Dubicka , Jarosław Tyszka, Agnieszka Pałczyńska, Michelle Höhne, Jelle Bijma, Max Janse, Nienke Klerks, Ulf Bickmeyer

Ecological Chemistry, Alfred-Wegener-Institut Helmholtz-Zentrum für Polar-und Meeresforschung, Bremerhaven D-27570, Germany • GFZ German Research Centre for Geosciences, Telegrafenberg, 14473 Potsdam, Germany • Faculty of Geology, University of Warsaw, Warsaw PL 02-089, Poland • Research Centre in Kraków, Institute of Geological Sciences, Polish Academy of Sciences, Kraków 31-002, Poland • Marine Biogeosciences, Alfred-Wegener-Institut Helmholtz-Zentrum für Polar-und Meeresforschung, Bremerhaven D-27570, Germany • Burgers' Ocean, Royal Burgers' Zoo, Arnhem 6816 SH, The Netherlands

 [https://en.wikipedia.org/wiki/Open\\_access](https://en.wikipedia.org/wiki/Open_access)

 Copyright information

## Abstract

Living organisms control the formation of mineral skeletons and other structures through biomineralization. Major phylogenetic groups usually consistently follow a single biomineralization pathway. Foraminifera, which are very efficient marine calcifiers, making a substantial contribution to global carbonate production and global carbon sequestration, are regarded as an exception. This phylum has been commonly thought to follow two contrasting models of either *in situ* “mineralization of extracellular matrix” attributed to hyaline rotaliid shells, or “mineralization within intracellular vesicles” attributed to porcelaneous miliolid shells. Our previous results on rotaliids along with those on miliolids in this paper question such a wide divergence of biomineralization pathways within the same phylum of Foraminifera. We found that both groups produced calcareous shells via the intravesicular formation of unstable mineral precursors (Mg-rich amorphous calcium carbonates) supplied by endocytosed seawater and deposited at the site of new wall formation within the organic matrix. Precipitation of high-Mg calcitic mesocrystals took place *in situ* and formed a dense, chaotic meshwork of needle-like crystallites. We did not observe deposition of calcified needles that had already precipitated in the transported vesicles, which challenges the previous model of miliolid mineralization. Hence, Foraminifera utilize less divergent calcification pathways, following the recently discovered biomineralization principles. Mesocrystalline chamber walls are therefore apparently created by accumulating and assembling particles of pre-formed liquid amorphous mineral phase within the extracellular organic matrix enclosed in a biologically controlled privileged space by active pseudopodial structures. Both calcification pathways evolved independently in the Paleozoic and are well-conserved in two clades that represent different chamber formation modes.

### eLife assessment

This manuscript provides **important** information on the calcification process, especially the properties and formation of freshly formed tests (the foraminiferan shells), in the miliolid foraminiferan species *Pseudolachlanella eburnea*. The evidence from the high-quality SEM images is **convincing** although the fluorescence images only provide indirect support for the calcification process.

<https://doi.org/10.7554/eLife.91568.2.sa3>

## Introduction

Over the past 500 million years, living organisms evolved different skeleton crystallization pathways. Very popular in nature is the mineralization of the extracellular matrix, for example, in crustacean cuticles, mollusk shells, vertebrate bones, and teeth composed of dentin and enamel (Weiner and Addadi, 2011 [↗](#); Kahil et al., 2021 [↗](#)). Radial foraminifera represented by rotraliids have been traditionally interpreted to make use of this crystallization mode (Weiner and Addadi, 2011 [↗](#)). The other two pathways are intravesicular and are characterized by either production of amorphous unstable phase within a large vesicle, such as a syncytium, well documented for sea urchin larvae (Beniash et al., 1997 [↗](#)) or crystallization of calcite elements within smaller vesicles located in the intracellular space, as seen in fish that form guanine crystals and coccolithophores to produce coccoliths (Weiner and Addadi, 2011 [↗](#); Kahil et al., 2021 [↗](#)). This model has also been attributed to the formation of porcelaneous shells by miliolid foraminifera (Weiner and Addadi, 2011 [↗](#)) based on the model proposed by Berthold (1976 [↗](#)) and followed by Hemleben et al. (1986 [↗](#)). As such, mineralization of shells in Foraminifera is believed to follow two highly contrasting pathways. The current theory states that Miliolida, characterized by imperforate, opaque milky-white shell walls (porcelaneous) (Angell, 1980 [↗](#); Hemleben et al. 1986 [↗](#); de Nooijer et al., 2009 [↗](#)), produce fibrillar crystallites composed of Mg-rich calcite within tiny vesicles enclosed by cytoplasm. Miliolid shells are made of randomly distributed calcite needles that form a dense meshwork of chaotic crystallites that cause light reflection, resulting in opaque (porcelaneous) milky walls (Hohenegger, 2009 [↗](#)). Calcite needles are thought to be precipitated completely within these vesicles and then transported to the site of chamber formation to be released via exocytosis (Berthold, 1976 [↗](#); Hemleben et al. 1986 [↗](#); Angell, 1980 [↗](#); de Nooijer et al., 2008 [↗](#), 2009 [↗](#)). The pre-formed needles or needle stacks are believed to be continuously embedded in an organic matrix in the shape of the new chamber until the wall is completed. Although this model is commonly accepted, it has never been sufficiently documented *in vivo*, and it does not resolve several conflicting issues. First of all, the question is how pre-formed bundles of parallel calcitic needles are transformed into randomly oriented needles within the shell wall. It is difficult to explain, if there is no recrystallization process within the wall structure after discharging the calcite crystallites. This problem was already emphasized by Hemleben et al. (1986 [↗](#)). Secondly, why the newly constructed wall is still translucent after deposition of random crystals. We would expect a thin milky opaque layer of the new wall under normal transmitted light, as well as polarized crystals of calcite under crossed nicols. Angell (1980 [↗](#)) on his plate 2 presenting porcelaneous chamber formation in miliolid *Spiroloculina hyalina* Schulze clearly documented the polarization front being shifted circa a half of the length of the new chamber behind the leading edge of the forming chamber. This shift represented more than an hour. Therefore, polarization was missing in the early and middle stage of chamber formation. It means that Angell's (1980) time lapse micrographs of the chamber formation were in conflict with the imaging under TEM. It seems that Angell (1980 [↗](#)) was aware of that problem and stressed that calcification had to be “intense enough to show under crossed nicols lags behind the leading edge

of the forming chamber” (p. 93, pl. 2 fig. 12/caption). In fact, all experiments that show the “crystal vacuoles” (sensu Angell, 1980) documented under TEM (Berthold, 1976; Hemleben et al. 1986; Angell, 1980) required fixation of the samples, which was prone to post-fixation artifacts of unwanted calcite precipitation.

Our goal is to test whether the miliolid shell is produced by “agglutination” of premade needle-like calcitic crystallites, and in consequence, whether this large group of calcareous Foraminifera follow crystallization within smaller vesicles located in the intracellular space. Therefore, we re-examined the mineralization process in Miliolida based on experiments on a living species, *Pseudolachlanella eburnea* (d’Orbigny) (Fig. 1). This taxon was selected to facilitate replicated observations of chamber growth under controlled culture conditions. We included observations of *in vivo* biomineralization using multiphoton and confocal laser scanning microscopy (CLSM) followed by analyses of fixed specimens at different stages of chamber formation by high-resolution field emission scanning electron microscopy (FE-SEM) coupled with energy dispersive X-ray spectrometry (EDS). Our new FE-SEM data challenge the current understanding of the biomineralization of miliolid foraminifera and such a significant divergence of biomineralization pathways within the Foraminifera.

## Results

All replicated *in vivo* experiments on *Pseudolachlanella eburnea* facilitated by CLSM imaging with the application of membrane impermeable Calcein and FM1-43 membrane dyes (performed in separate experiments) showed intravesicular fluorescence signals from groups of moving vesicles (1–5 μm in size) inside the cytosol (Fig. 2A, B, Movies S1 and S2). The fluorescent vesicles inside the cytosol contained seawater, as documented by fluorescence of membrane impermeable Calcein. These vesicles were taken up by endocytosis indicated by FM1-43 staining. This dye stains the cell membranes and indicates all endocytic vesicles by fluorescence, whereas the other intracellular vesicles remain unstained (Amaral et al., 2011). Both dyes demonstrate the uptake of seawater via the endocytosis of vesicles that are approximately 1–4 μm in diameter and move through the entire cell.

Additional LysoGlow84 staining revealed numerous acidic vesicles in the cytosol the presence of (Fig. 2C, Movies S3 and S4). Acidic vesicles were accompanied by other vesicles (approximately 1–2 μm in size) that show autofluorescence upon multiphoton excitation at 405 nm (emission 420–480 nm), shown in red in Figure 2C. This wavelength partly permeates the shell to excite autofluorescence interpreted as associated with ACCs (see Dubicka et al., 2022). The autofluorescence of the shell itself is also present (Figure 2D), however, it is not clearly visible because the fluorescence of ACCs is much stronger. The intensity of the laser light is reduced because the multiphoton light has to pass through a thick three-dimensional carbonate wall of the foraminiferal shell. Further experimental studies are needed to confirm the ACC source of this autofluorescence and thus definitively eliminate potential organic sources of AF emissions.

In addition, typical chlorophyll autofluorescence (excitation at 405 or 633 nm, emission 650–700 nm, Fig. 2C, Movies S3 and S4 highlighted in green) was detected, which indicated the presence of chloroplasts in microalgae cells. These algal cells have been found to move within the cytosol of the observed specimens, in proximity of acidic vesicles and vesicles characterized by autofluorescence upon UV light (ex. 405 nm). These algal cells may represent facultative endosymbionts, as they were observed only during the chamber mineralization process in specimens with carbonate-bearing vesicles detected by *in vivo* CLSM experiments. They were documented just below the organic matrix (OM) of the newly formed chamber, as seen in the FE-SEM observations as well as just below the organic matrix (OM) of the newly created chamber as seen in the FE-SEM observations (Figs. S1G, and S1H).

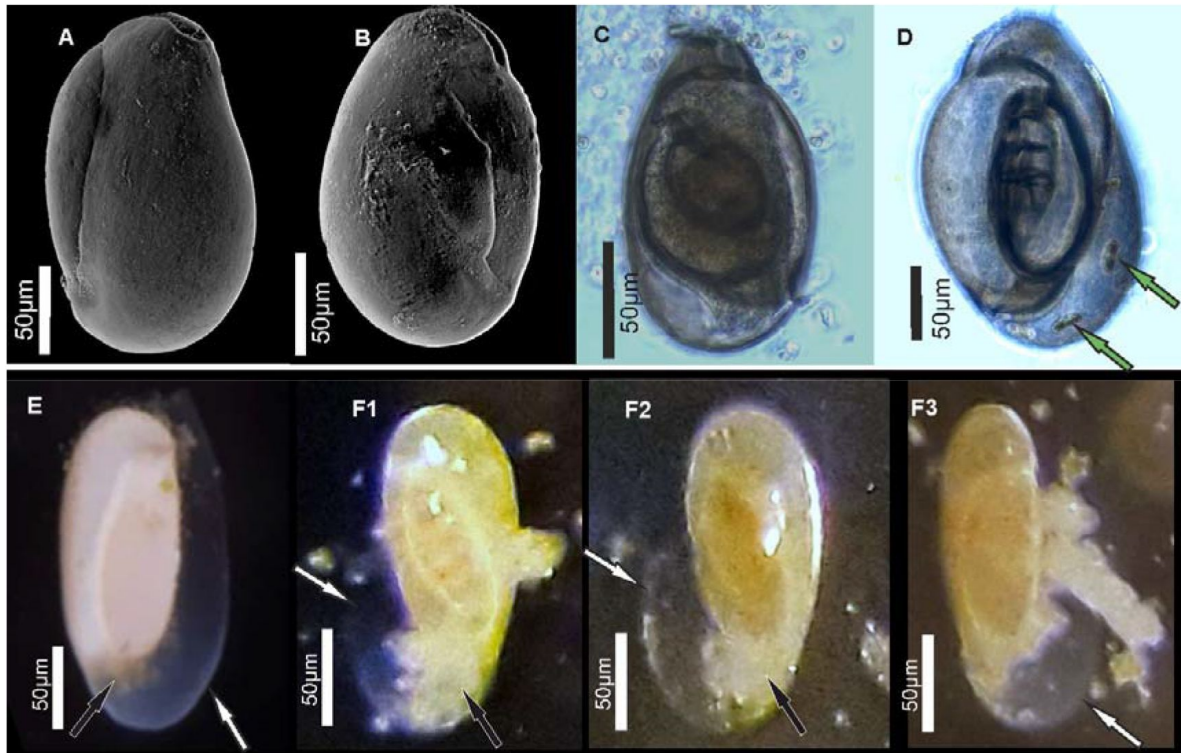


**Figure 1.**

Specimens of miliolid foraminifera, identified as *Pseudolachlanella eburnea* (d'Orbigny), used for experimental studies. (A, B) SEM, (C, D) transmitted light microscope, and (E, F) stereomicroscope images. White arrows show the outer organic sheath of a new chamber during its gradual calcification expressed by its gradual appearance from complete transparency to milky and opaque aspect (E, F). Black arrows indicate a small mass of cytoplasm extruded from the aperture of exiting the chamber. Green arrows point to incorporated algae.



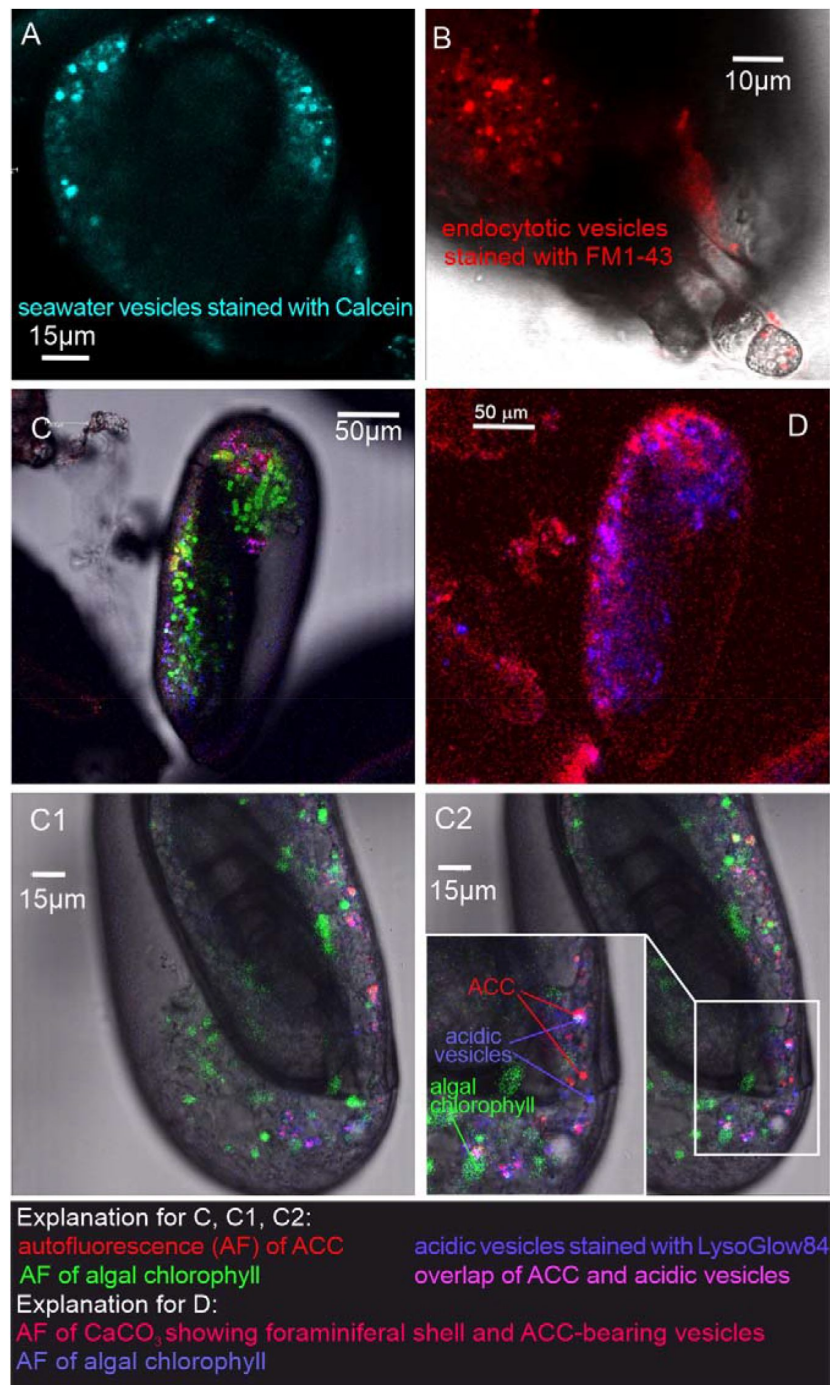


**Figure 2.**

Fluorescence images of living *P. eburnea* conducted by Laser Scanning Microscopy. A - Cell impermeable Calcein (cyan) indicating endocytotic seawater vesicles, see Movie 1. B - FM1-43 membrane dye indicating endocytotic vesicles (red), see Movie 2. C, E - LysoGlow84 indicating acidic vesicles (navy blue), autofluorescence of chloroplasts (green), and Mg-ACC pools (red), see Movies 3 and 4, (note the overlap of ACC and acidic vesicles is marked in lilac). D - Autofluorescence image with reduced threshold of the studied Miliolida species (exc. 405 nm) showing algal chlorophyll (blue) and CaCO<sub>3</sub> (red), both ACC and calcite shell.

Specimens of *P. eburnea*, which displayed vesicles showing autofluorescence under UV light inside the cytosol, were fixed using Method B (see Materials and Methods) coated with a few nanometers of carbon and analyzed by SEM-EDS. The main elements detected in the area of the fixed cytoplasm (Fig. S4) were C, O, Na, Mg, P, S, Cl, K, and Ca (of particular interest were the high contents of Mg and Ca), whereas the main elements detected within the area of the new chamber in the form of a gel-like matter filled with dispersed nanograins were C, O, Na, Mg, S, Cl, and Ca (Fig. S4). The shell content was strongly enriched with Ca relative to the cytoplasm, which showed a much higher Mg/Ca ratio.

FE-SEM observations of the fully mineralized test walls displayed the porcelaneous structures (see Parker, 2017 [↗](#); Dubicka et al., 2018 [↗](#)), which are made of three mineralized zones, i.e. (I) extrados that represents an outer mineralized surface (approximately 200–300 nm in thickness; Figs. S1C and S2C); (II) porcelain that denotes the main body of the wall constructed from randomly oriented needle-shaped crystals (up to 1–2 μm in length and approximately 0.2 μm in width). No gel-like matter was observed between the needles of the porcelain structures that appeared in the early stages of wall formation (Figs. 3E; 3E1 [↗](#); S2C, and S3A); and (III) intrados that represents an inner mineralized surface (approximately 200–300 nm in thickness) made of needle-shaped crystallites (Figs. 3E, 3E1 [↗](#) and S1A).

Growing chambers, captured at the various successive stages of chamber formation in different specimens, have revealed the following morphological features: (A) a solitary, thin organic sheath (approximately 200–300 nm thick) that represents the most distal part of the new chamber and is anchored to the older, underlying solid calcified chamber (Fig. 4A [↗](#)); (B) a solitary, outer organic sheath (OOS) filled with spread calcifying nanograins (Figs. 4B [↗](#); S2A, and S2B); (C) a gel-like matter (4–5 μm in thickness) with a granular texture, bounded on two sides by intrados and extrados, and containing relatively widely spaced, randomly dispersed carbonate nanograins (Figs. 3A–B [↗](#); 4C [↗](#); S1A–D); (D) the test inside made of chaotic meshwork of carbonate nanograins partly transformed to short needles with a small amount of gel-like OM in-between (Figs. 3C, D [↗](#), and 4D [↗](#)); (E) the test inside composed of needle-shaped crystals with planar faces and no apparent remaining gel-like matter (Figs. 3E, E1 [↗](#) and 4E [↗](#)). Carbonate nanograins at the shell construction site were well documented in our SEM-EDS studies (Fig. S4). Both fixation methods (see Material and Methods) yielded highly consistent results.

## Discussion

### Porcelaneous shell formation

Comparative analysis of the nanostructures of the newly built chambers combined with the elemental composition obtained from SEM-EDS, as well as the data from CLSM, allowed us to identify important steps in the accretive formation of *P. eburnea* shells. The formation of a new chamber begins with the construction of a thin outer organic sheath (OOS) that pre-shapes the new chamber (Figs. 4A [↗](#), 5 [↗](#)). The outer organic sheath is made by pseudopodial structures supported by the cytoskeleton immediately after the extrusion of a small mass of cytoplasm from the aperture (Figs. 1E [↗](#), and 1F [↗](#)). Once the OOS is constructed, the first calcium carbonate accumulation takes place inside in the form of carbonate nanograins (Figs. 4B [↗](#), 5 [↗](#), S2A and S2B), creating the extrados. The extrados stabilizes the final chamber morphology relatively quickly. Subsequently, the wall gradually thickens through the primary accumulation of hydrated and amorphous Mg-rich CaCO<sub>3</sub> (Figs. 4B [↗](#), 5 [↗](#)). We suppose that the carbonate content is successively deposited by exocytosis of Mg-ACC rich vesicles that most likely represent the vesicles converted from seawater stained with Calcein (Fig. 5 [↗](#)). The characteristic autofluorescence inside foraminiferal cell excited at 405 nm (Fig. 2 [↗](#); Movies S3 and S4) most likely indicates the carbonate content of the vesicles, which are considered to be Mg-ACCs (see Dubicka et al., 2023 [↗](#)). Mg-ACC is an unstable, amorphous and hydrated form of CaCO<sub>3</sub> with a significantly high

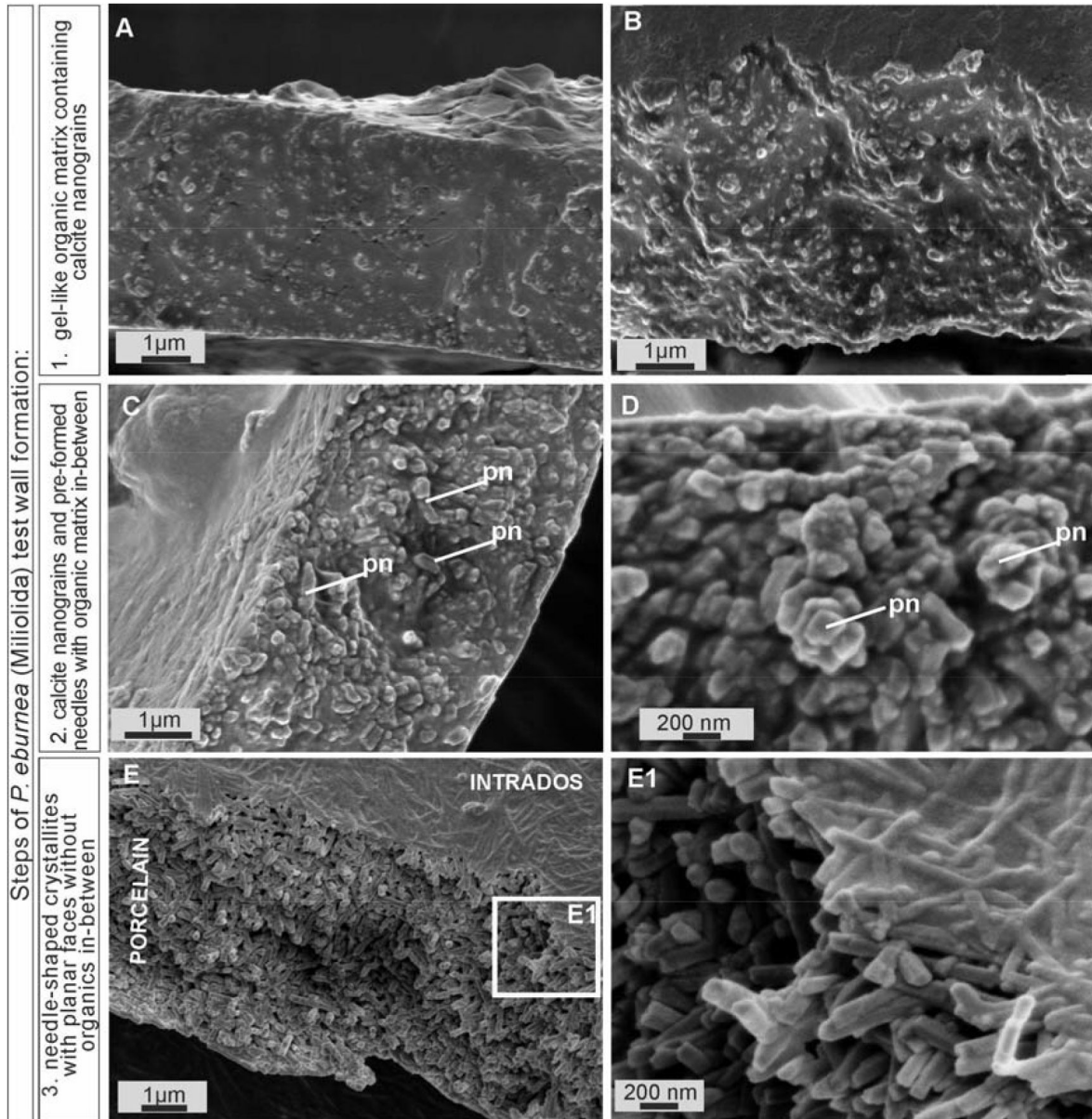


**Figure 3.**

SEM images of the major steps of the formation of *P. eburnea* shell-building components. Test cross-section showing: (A, B) carbonate nanograins within organic matrix, (C, D) nanograins merging into needle-like mesocrystals, (E) fully developed needle-shaped elements; pn -nanograins partly transformed to short needles.



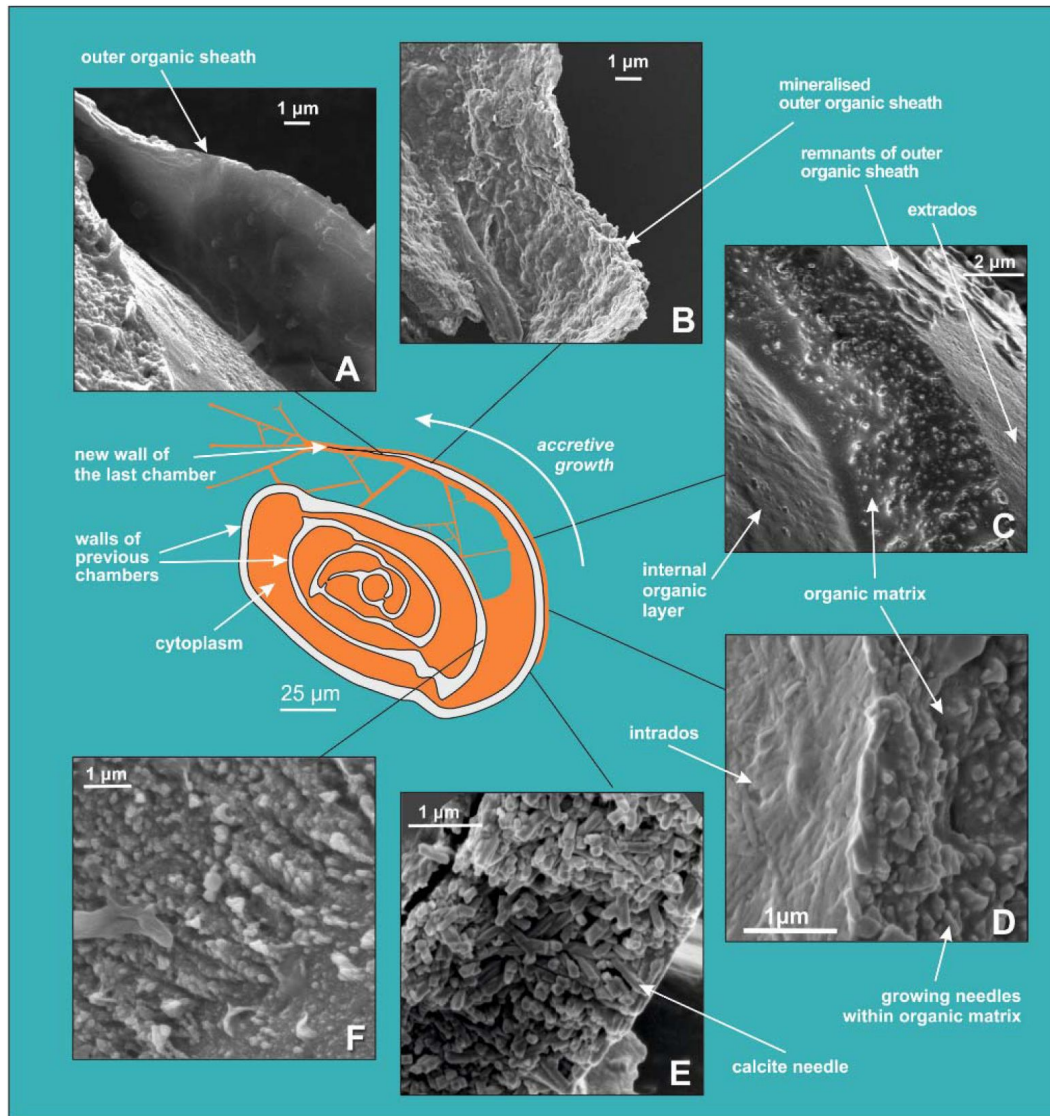


**Figure 4.**

SEM images showing successive stages of new chamber formation in *P. eburnea*. (A) outer organic sheath, (B) mineralized outer organic sheath, (C) calcite nanograins within a gel-like organic matrix, (D) needle-shaped mesocrystal growth, (E) needle-like calcite building elements, (F) nanogranular intrados.



concentration of Mg (Raz et al., 2000 [↗](#); Weiner et al., 2003 [↗](#); Bentov and Erez, 2006 [↗](#); Kahil et al., 2021 [↗](#)) and is commonly regarded as a resource for most biocalcification processes. ACCs have been found in many calcifying marine organisms, such as echinoderms, mollusks, coccolithophorid algae, cyanobacteria, crustaceans, and rotraliid foraminifera, where they are typically interpreted as pre-material phases for the production of calcite skeletons (Hasse, et al., 2000 [↗](#); Weiss et al., 2002 [↗](#); Sviben et al., 2016 [↗](#); Dubicka et al., 2018 [↗](#); Kahil et al., 2021 [↗](#)). Research suggests that a high Mg content not only makes ACC unstable but also facilitates the transport of ACC to the crystallization site, where it is initially transformed into carbonate nanograins (Cölfen and Qi, 2001 [↗](#); Addadi and Weiner, 2003; Raz et al., 2003 [↗](#); Dubicka et al., 2023 [↗](#)). The existence of intracellular, vesicular intermediate amorphous phase (Mg-ACC pools), which supplies successive doses of carbonate material to shell production, might be supported not only by autofluorescence (excitation at 405 nm; **Fig. 2** [↗](#); Movies S3 and S4; see Dubicka et al., 2023 [↗](#)) but also by a high content of Ca and Mg analyzed in the cytoplasmic area by SEM-EDS analysis (Fig. S4). In the future, more precise higher resolution elemental measurements are needed for better documentation of miliolid ACC-bearing vesicles. However, the small size of carbonate-bearing vesicles (approximately 1–2  $\mu\text{m}$ ) may make this difficult.

$\text{Mg}^{2+}$  and  $\text{Ca}^{2+}$  ions for intravesicular production of Mg-ACCs are obtained from seawater and taken up by endocytosis, as independently indicated by membrane impermeable Calcein, as well as by the FM1-43 probe selectively labelling membranes of endocytic vesicles (**Fig. 2A, B** [↗](#), Movies S1 and S2). We hypothesize that vesicles are carried along cytoskeletal structures to the OM, as observed in rotraliid foraminifera (Dubicka et al., 2023 [↗](#)), where they dock and release their contents (**Fig. 4** [↗](#)). The nanograins then precipitate within the gelatinous matter that consists of amorphous carbonates and organic matrix released from the vesicles (**Figs. 3A-C** [↗](#), **4C** [↗](#), and **5** [↗](#)). Nanograins immersed in the gel-like matter gradually grow into needle-shaped elements, precipitating *in situ* within the final wall structure (**Figs. 3C, 3D** [↗](#), and **4D** [↗](#)). The gel-like matter appears to be involved in needle formation; however, the OM seems to disappear (**Figs. 3E** [↗](#) and **4E** [↗](#)) when the needle-shaped crystals are created. We suspect that the gel-like matter consists of pre-formed liquid amorphous mineral phase (Mg-ACC) within the extracellular organic matrix that is suggested by the EDS spectra of the early stage of the wall calcification (Fig. S4: A3 area). The calcification of extrados and intrados occurs before the interior of the wall crystallizes, providing stability to the new chamber at both edges of the wall (**Fig. 4D** [↗](#)).

The protruding cytoplasm appears to immediately form a chamber wall by secreting OM and crystals from the vesicles (Angell, 1980 [↗](#)). As calcite secretion continues along the leading edge, the newly formed segment remains covered by a thin, moving sheet of cytoplasm that is called by Angell (1980 [↗](#)) the “active sheet”. This thin active sheet of cytoplasm may represent a lamellipodium that is a pseudopodial structure known to be involved in the biomineralization of Rotaliida (Tyszka et al., 2019 [↗](#)). It is also likely that reticulopodial structures (that do not coat the whole calcification site) are responsible for the distribution and shape of the internal surface of the chamber wall. That occurs by successive accumulation of ACC and OM as identified on TEM images by Angell (1980 [↗](#); p. 97). His results suggest that crystallization of calcite needles is “limited to a confined space controlled by active cytoplasmic structures” that are strictly separated by the membranes from the cytosol.

## Formation of shell crystallites: A paradigm shift

Miliolids were thought to share a similar, intracellular, crystallization pathway as the coccolith formation in coccolithophorids (Weiner and Addadi, 2011 [↗](#)) that evolved in the Triassic, that is c. 210 Myr ago (Gardin et al., 2012 [↗](#)). Coccoliths are produced within intracellular Golgi-derived vesicles and then exported to the surface of the extracellular coccosphere (de Vrind-de Jong et al., 1986 [↗](#)). Miliolids, with their unique fibrillar calcitic microstructures, evolved much earlier, that is ca. 300 Myr ago in the late Paleozoic (Fig. S5). Until now, it was generally considered that miliolid crystals also precipitate within vesicles immersed in the cytoplasm and are then transported to the location of the wall construction, where they are released by exocytosis (Berthold, 1976 [↗](#); Angell,

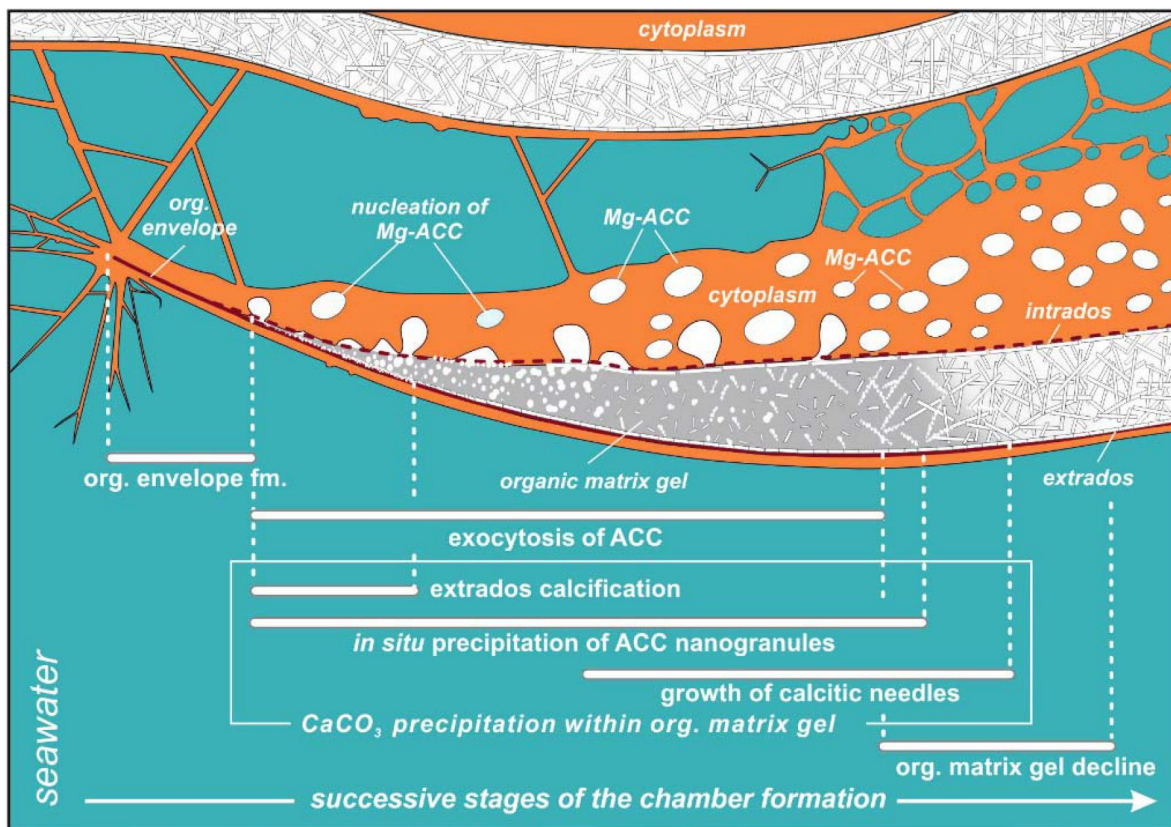


**Figure 5.**

Simplified model of porcelaneous wall construction based on foraminifer *P. eburnea*. White spots labeled as Mg-ACC represent vesicles with Mg-rich amorphous calcium carbonates.

1980 [↗](#); de Nooijer et al., 2009; Hemleben et al., 1986 [↗](#); Weiner and Addadi, 2011 [↗](#)). Our FE-SEM study of *P. eburnea* shows the lack of premade needle-like crystallites of calcite at the early stages (I-IV) of the wall formation. In contrast, we can clearly infer the *in situ* calcification front with a progressive sequence of crystal growth behind the leading edge of the forming chamber (Figs 4 [↗](#), 5 [↗](#)). Therefore, this miliolid species apparently does not produce shells by “agglutination” of premade needle-like crystallites of calcite, in contrast to the traditional miliolid calcification model (Berthold, 1976 [↗](#); Angell, 1980 [↗](#); Hemleben et al., 1986 [↗](#)).

In the light of these results, another argument emerges that further confirms *in situ* calcification of miliolid chambers. It explains the extended transparency of unmineralized walls observed under the light stereomicroscope. The chamber wall under formation tends to gradually change its appearance during calcification from completely transparent to milky and opaque (Fig. 1E, F [↗](#)).

Our results on biomineralization of this miliolid species do not confirm the formation of individual skeletal crystallites within intracellular vesicles. However, in turn, our results do support existence of endocytotic vacuolization of sea water in miliolids that was first suggested by Hemleben et al. (1986) [↗](#). We further support Angell’s (1980) interpretation that the calcite crystals are dispersed in the gel-like organic matrix (see Figs 3A, B [↗](#); 4C, D [↗](#); 5 [↗](#)). This gel-like fluidal organic matrix most likely include a rich Mg-ACC component as the substrate for *in situ* calcification (Figs 3 [↗](#)-5 [↗](#)). Interestingly, the previous studies by Angell (1980) [↗](#) did not support crystal formation within vacuoles either.

Precipitation of calcite nanograins, which then merge and transform into crystallites, occurs within the organic matter after the release of Mg<sup>2+</sup> from Mg-ACC. The organic matter provides an appropriate physiochemical microenvironment for initiating and maintaining the crystallization process by manipulating many essential factors including pH, and kinetics of the system (Kahil et al., 2021 [↗](#)). According to Tyszka et al. (2021) [↗](#), the organic matrix involved in the biomineralization of foraminiferal shells may contain collagen-like networks.

Our *in vivo* CLSM observations show a miliolid cytoplasm containing intracellular carbonate-bearing vesicles. Such vesicles have been well-documented by Angell (1980) [↗](#), who stressed their crucial role in the biomineralization process. However, rather than transporting pre-formed solid needles, the vesicles likely carry liquid or quasi-liquid calcification substrates. The liquid phase of the ACC apparently was maintained by a relatively high concentration of Mg (S4), which was much higher than that in the shell, as detected by the SEM-EDS analyses.

Recently, an independent study was performed on another miliolid species - *Sorites orbiculus* (Nagai et al., 2023 [↗](#)). The researchers reported highly complementary results that indicate the lack of crystal-like structures within the intracellular vesicles. Their results suggested that calcification of this miliolid species did not follow Hemleben’s et al (1986) [↗](#) model because intracellular vesicles did not produce needle-like crystals to construct the shell wall. They also stated that their observations “may reveal a novel and unknown mode of biomineralisation in foraminifera”.

Because, miliolid wall texture originated together with the appearance of miliolid foraminifera as it has also been recorded within Paleozoic taxa (Fig. S5) thus the calcification mode of miliolids apparently evolved in the late Paleozoic (≥ 350 Mya) and is well conserved in this clade till today. It should be emphasized that our recent understanding of all calcification pathways in Foraminifera implies their independent evolution within main phylogenetic groups, besides miliolids and rovaliids, also including spirillinids, nodosariids, and robertinids (Mikhalevich, 2004; Pawlowski et al., 2013 [↗](#); Mikhalevich, 2014; Dubicka et al., 2018 [↗](#); Dubicka, 2019 [↗](#); Mikhalevich, 2021; Sierra et al., 2022; de Nooijer et al., 2023). In fact, most of these biomineralization evolutionary transitions from agglutination to calcification originated in the mid and late Paleozoic. Mg-ACC has also recently been documented in rovaliid foraminifera (Dubicka et al., 2023 [↗](#)). Therefore, the

biocalcification processes in Rotaliida and Miliolida, which belong to the two main foraminiferal classes Globothalamea and Tubothalamea, respectively (Pawlowski et al., 2013), are more similar than previously thought (Weiner and Addadi, 2011). Their mesocrystalline chamber walls are created by accumulating and assembling particles of pre-formed liquid amorphous mineral phase. Their calcification occurs within the extracellular organic matrix enclosed in a biologically controlled privileged space by active pseudopodial structures. However, we are aware that this process must also vary to some extent as the chemical composition of the calcite, as well as primary crystallite geometries differ between the groups. Seawater provides the relevant Ca and Mg ions for calcification, which are taken up in both groups by endocytosis. In *Amphistegina* (Rotaliida), this process is performed by shell pores (Dubicka et al., 2023), as well as apertures and foramina; in non-porous Miliolida, it is done by granuloreticulopodia emanating from the aperture (Fig. 2, Movie S2). In both the rotaliid *Amphistegina* and the miliolid *P. eburnea* carbonate-bearing vesicles are surrounded by moving acidic vesicles (Fig. 2, Movies S3 and S4), which likely facilitate pH regulation at the mineralization front (see Toyofuku et al., 2017; Chang et al., 2023). It is very likely that pH is controlled by active outward proton pumping by a V-type H<sup>+</sup> ATPase or proton outflux driven by pH that is responsible for the proton flux and related calcification (Toyofuku et al., 2017; see also Matt et al., 2022). We suspect much higher pH values within vesicles transporting Mg-ACC to the site of calcification. Such alkaline vesicles were detected by the HPTS fluorescent labelling and reported by several previous studies (de Nooijer et al., 2008; 2009).

Our findings are in line with recent work in biomineralization, supporting that “biominerals grow by the accretion of amorphous particles, which are later transformed into the corresponding mineral phase” (Macías-Sánchez et al., 2011, p. 1; see also Meldrum and Cölfen, 2008). Miliolid needles, assembled with calcite nanoparticles, are unique examples of biogenic mesocrystals (see Cölfen and Antonietti, 2005), as they form distinct geometric shapes limited by planar crystalline faces. Mesocrystals are constructed from highly ordered individual nanoparticles (Cölfen and Mann, 2003; Strum and Cölfen, 2016; 2017) that form hierarchically structured solid materials in the crystallographic register and are rather devoid of outer planar surfaces. These result from the aggregation, self-assembly, and mesoscopic transformation of amorphous precursor nanoparticles. Mesocrystals are common biogenic components in the skeletons of marine organisms, such as corals, echinoderms, bivalves, sea urchins, and rotaliid foraminifera (e.g., Macías-Sánchez et al., 2011; Benzerara et al., 2011; Seto et al., 2012; Evans et al., 2019; Dubicka et al., 2023).

Our biomineralization model further explains the random orientation pattern of the calcite needles within the shell wall. The miliolid intertwined calcitic structure cannot be explained by the models proposed by Berthold (1976) and followed by Hemleben (1986), that is, by the successive deposition of vesicles with ready bundles of solid calcitic fibers (needles) without additional recrystallization processes. In our proposed *in situ* calcification model, calcite crystallites have sufficient space to grow within the flexible gelatinous organic matrix. In addition, our model explains the need for a light and dark phase for the algae that are present inside *P. eburnea* during the biomineralization processes, as these algae possibly play an important role. Small miliolid coiling foraminifera has been regarded as a non-symbiotic taxon because their shells are not transparent, however, this is not true for red and infrared light. Fully developed miliolid shells are made of randomly distributed needles that cause light reflection, resulting in opaque (porcelaneous) walls that possibly protect the foraminifera from UV irradiation and allow them to live in extremely illuminated shallow seas (Hohenegger, 2009). These walls are permeable to red and infrared light, as we observed using multiphoton laser. Red light is commonly believed to be the most efficient waveband for photosynthesis however green light may achieve higher quantum yield of CO<sub>2</sub> assimilation and net CO<sub>2</sub> assimilation rate (Liu and Lerser, 2021). *Pseudolachlanella eburnea* may acquire its facultative symbionts only for the duration of the biomineralization process. The late stage of needle formation in the shell production process ensures that the wall remains transparent by the time the needles are completed. Similar patterns of the gradual change from transparent to opaque whitish walls were also observed in larger



symbiotic miliolids by Marshalek (1969), Wetmore (1999), and Tremblin et al. (2022). The latter authors (Tremblin et al., 2022) documented chamber formation of miliolid *Vertebralina striata* with cytoplasm enveloped by a transparent sheath decorated with striate already present in the transparent wall before calcification. They also interpret white areas on the sheath, indicating incipient concentrations of minute calcite crystallites that represent the mineralised wall. The biomineralization process is likely aided by their dark respiratory activity (see Hallock, 1999 [↗](#)), as they could supply calcification substrates such as  $\text{HCO}_3^-$  through respiration or by increasing pH at the calcification site during the light phase. Similarly, representatives of miliolid large benthic foraminifera (Archaiasidae, Soritidae, and Peneroplidae) host endosymbiotic algae (Lee, 2006 [↗](#); Prazes and Renema, 2019). Therefore, they have developed additional morphological and textural features such as pits, grooves/striate, or windows, which enable light penetration into the places where symbionts are positioned (see Hohenegger, 2009 [↗](#), Parker 2017 [↗](#)).

## Materials and Methods

Living foraminifera, collected from the coral reef aquarium in the Burgers' Zoo (Arnhem, Netherlands), were cultured in a 10 L aquarium containing seawater with a salinity of 32‰, pH of 8.2, and a temperature of 24 °C. *Pseudolachlanella eburnea* (d'Orbigny) was placed in 4 mL petri dishes one day before CLSM studies and observed under a Zeiss Stemi SV8 Stereomikroskop. Selected individuals were studied *in vivo* using a Leica SP5 Confocal Laser Scanning Microscope equipped with an argon, helium-neon, neon, diode, and multiphoton Mai Tai laser (Spectra-Physics) at the Alfred-Wegener-Institut, Bremerhaven, Germany. *In vivo* experiments were performed by labeling samples with different fluorescent dyes (**Table 1** [↗](#)) just before imaging using, pH-sensitive LysoGlow84 (50 μM exc. MP720 nm exc/em. 380–415 nm and 450–470 nm, Marnas Biochemicals Bremerhaven, incubation time: 2 h), FM1-43 membrane stain (1 μM, exc. 488 nm em. 580–620 nm, Invitrogen, incubation time: 24 h), and membrane impermeable Calcein (0.7 mg/10 mL, exc. 488 nm, em. 510–555 nm, incubation time: 24 h). The foraminifera were removed from the Petri dish with clean water using a pipette. In addition, the autofluorescence of specific foraminiferal structures at the chosen excitation/emission wavelength was detected. All experiments were replicated with at least several individuals of the same species. All fluorescence probe experiments were performed with appropriate controls.

Additional foraminifera individuals that had been studied by CLSM were fixed for further analysis. The fixation process followed two different methods: (A) 60 individuals were transferred to 3% glutaraldehyde for 5 s and then dehydrated stepwise for a few seconds with an ethanol/distilled water mixture with increasing concentrations (30%, 50%, 70%, and 99%). (B) The seawater was removed from 50 individuals by pipetting and applying a small piece of Kimtech lab wipe (without any rinsing), followed by quick drying in warm air (30–35 °C). This method stops the dissolution of the amorphous mineral phase because there is no contact with other liquids. Fixed foraminifers of both procedures were gently broken using a fine needle to coat the cross-sectional surfaces and tested inside with a few nanometers of either gold or carbon. Foraminifera were then studied using a Zeiss Sigma variable-pressure field-emission scanning electron microscope (VP-FESEM) equipped with EDS at the Faculty of Geology, University of Warsaw.

## Acknowledgements

This work was supported by the Alexander von Humboldt Foundation Research Fellowship for experienced researchers to Z.D. and the Polish National Science Center (UMO-2018/29/B/ST10/01811) to J.T. and Z.D., a grant coordinated by Grzegorz Racki, University of Silesia. We thank Oscar Branson for his comments on an earlier version of the manuscript and the suggested improvements.

dye	concentration	excitation nm	emission nm	source	function
Lysoglow84	50µM	Multiphoton 730	380-415/450-470	Marnas Biochemicals	pH, membrane permeable
FM1-43	1µM	Argon 488 or Multiphoton 1000nm	580-620	Thermo Fisher Scientific	Membrane staining
Calcein	0,7mg/10mL	Argon 488	510-555	Thermo Fisher Scientific	Membrane impermeable water soluble dye
autofluorescence		Diode 405 MP 800	420-490		CaCO <sub>3</sub> , ACC
autofluorescence		Diode 405/ HeNe 633	650-700		Chlorophyll of algae

**Table 1.**

**Wavelengths and dyes**

## Movie captions

**Movie S1 (separate file).** Living *P. eburnea* showing cell impermeable Calcein (blue, exc. 488nm em. 505-555) in a series of 107 overlaid images taken during 428 s. Calcein staining indicates the occurrence of seawater vesicles inside the cytosol.

**Movie S2 (separate file).** FM1-43 membrane probe fluorescent signals (red, exc. 488nm, em. 580-620nm) emitted by intracellular vesicles within cytosol of *P. eburnea*. Because FM1-43 stains only the cell membrane, the observed vesicles must be originated during the process of endocytosis. The movie was taken by overlaid of 84 images during 433 s.

**Movie S3 (separate file).** Living *P. eburnea* showing fluorescence signal inside the cytosol: autofluorescence of Mg-ACC pools (red, exc. 405nm, em. 420-490nm) and algal chloroplasts (green, exc. 633nm, em. 640-690nm), fluorescent signal of LysoGlow84 pH sensitive dye (exc. MP 720nm, em. 440-470nm) indicating acidic vesicles. The movie was taken by overlaid of 37 images during 555 s.

**Movie S4 (separate file).** Living *P. eburnea* showing fluorescence signal inside the cytosol: autofluorescence of Mg-ACC pools (red, exc. 405nm, em. 420-490nm) and algal chloroplasts (green, exc. 633nm, em. 640-690nm), fluorescent signal of LysoGlow84 pH sensitive dye (exc. MP 720nm, em. 440-470nm) indicating acidic vesicles. The movie was taken by overlaid of 37 images during 555 s.

## References

- Addadi L, Raz S, Weiner S (2003) **Taking advantage of disorder: amorphous calcium carbonate and its roles in biomineralization** *Advanced Materials* **15**:959–970 <https://doi.org/10.1002/adma.200300381>
- Amaral E, Guatimosim S, Guatimosim C (2011) **Using the fluorescent styryl dye FM1-43 to visualize synaptic vesicles exocytosis and endocytosis in motor nerve terminals** *Methods in Molecular Biology* **689**:137–48 [https://doi.org/10.1007/978-1-60761-950-5\\_8](https://doi.org/10.1007/978-1-60761-950-5_8)
- Angell W (1980) **Test morphogenesis (chamber formation) in the foraminifer Spiroloculina hyalina Schulze** *Journal of Foraminiferal Research* **10**:89–101
- Beniash E, Aizenberg J, Addadi L, Weiner S (1997) **Amorphous calcium carbonate transforms into calcite during sea urchin larval spicule growth** *Proceeding of the Royal Society London B* **264**:461–465 <https://doi.org/10.1098/rspb.1997.0066>
- Bentov S, Erez J (2006) **Impact of biomineralization processes on the Mg content of foraminiferal shells: A biological perspective** *Geochemistry, Geophysics, Geosystems* **7** <https://doi.org/10.1029/2005GC001015>
- Benzerara K, Menguy N, Obst M, Stolarski S, Mazur M, Tyliszczak T, Brown GE., Meibom A (2011) **Study of the crystallographic architecture of corals at the nanoscale by scanning transmission X-ray microscopy and transmission electron microscopy** *Ultramicroscopy* **111**:1268–1275 <https://doi.org/10.1016/j.ultramic.2011.03.023>
- Berthold WU (1976) **Biomineralisation bei milioliden Foraminiferen und die Matrizen-Hypothese** *Naturwissenschaften* **63**
- Chang WW, Thies AB, Tresguerres M, Hu MY (2023) **Soluble adenylyl cyclase coordinates intracellular pH homeostasis and biomineralization in calcifying cells of a marine animal** *Am J Physiol Cell Physiol* **324**:C777–C786 <https://doi.org/10.1152/ajpcell.00524.2022>
- Cölfen H, Qi L (2001) **A systematic examination of the morphogenesis of calcium carbonate in the presence of a double-hydrophilic block copolymer** *Chemistry—A European Journal* **7**:106–116 [https://doi.org/10.1002/1521-3765\(20010105\)7:1<106::aid-chem106>3.0.co;2-d](https://doi.org/10.1002/1521-3765(20010105)7:1<106::aid-chem106>3.0.co;2-d)
- Cölfen H, Antonietti M (2005) **Mesocrystals: Inorganic Superstructures Made by Highly Parallel Crystallization and Controlled Alignment** *Angew. Chem. Int* **44**:5576–5591 <https://doi.org/10.1002/anie.200500496>
- Cölfen H, Mann S (2003) **Higher-order organization by mesoscale self-assembly and transformation of hybrid nanostructures** *Angew. Chem. Int. Edit* **42**:2350–2365 <https://doi.org/10.1002/anie.200200562>
- Debenay J-P, Guillou J-J, Geslin E, Lesourd M (2000) **Crystallization of calcite in foraminiferal tests** *Micropaleontology* **46**:87–94



- Dubicka Z (2019) **Chamber arrangement versus wall structure in the high-rank phylogenetic classification of Foraminifera** *Acta Palaeontologica Polonica* **64**:1–18 <https://doi.org/10.4202/app.00564.2018>
- Dubicka Z, Bojanowski MJ, Bijma J, Bickmeyer U (2023) **Mg-rich amorphous to Mg-low crystalline CaCO<sub>3</sub> pathway in foraminifera** *Heliyon* **9** <https://doi.org/10.1016/j.heliyon.2023.e18331>
- Dubicka Z, Owocki K, Gloc M (2018) **Micro- and nanostructures of calcareous foraminiferal tests: insight from some representatives of Miliolida, Rotaliida and Lagenida** *Journal of Foraminiferal Research* **48**:142–155 <https://doi.org/10.2113/gsjfr.48.2.142>
- Erez J (2003) **The source of ions for biomineralization in foraminifera and their implications for paleoceanographic proxies** *Reviews in Mineralogy and Geochemistry* **54**:15–149 <https://doi.org/10.2113/0540115>
- Evans JS (2019) **Composite Materials Design: Biomineralization Proteins and the Guided Assembly and Organization of Biomineral Nanoparticles** *Materials* **12** <https://doi.org/10.3390/ma12040581>
- Gardin S, Krystyn L, Richoz S, Bartolini A, Galbrun B (2012) **Where and when the earliest coccolithophores?** *Lethaia* **45**:507–523 <https://doi.org/10.1111/j.1502-3931.2012.00311.x>
- Hallock P (1999) **Symbiont-bearing foraminifera** *In: Modern foraminifera Springer* :123–139
- Hasse B, Ehrenberg H, Marxen JC, Becker W, Epple M (2000) **Calcium carbonate modifications in the mineralized shell of the freshwater snail *Biomphalaria glabrata*** *Chemistry–A European Journal* **6**:3679–3685 [https://doi.org/10.1002/1521-3765\(20001016\)6:20<3679::AID-CHEM3679>3.0.co;2-#](https://doi.org/10.1002/1521-3765(20001016)6:20<3679::AID-CHEM3679>3.0.co;2-#)
- Ch Hemleben, Anderson OR, Berthold WU, Spindler M, Leadbeater B.C., Riding R. (1986) **Calcification and chamber formation in Foraminifera–A brief overview** *Biomineralization in Lower Plants and Animals* :237–249
- Hohenegger J (2009) **Functional shell geometry of symbiont-bearing benthic foraminifera** *Galaxea Journal of Coral Reef Studies* **11**:81–89 <https://doi.org/10.3755/galaxea.11.81>
- Hu MY, Petersen I, Chang WW, Blurton C, Stumpp M (2020) **Cellular bicarbonate accumulation and vesicular proton transport promote calcification in the sea urchin larva** *Proceedings of the Royal Society B* **287** <https://doi.org/10.1098/rspb.2020.1506>
- Kahil K, Weiner S, Addadi L, Gal A (2021) **Ion Pathways in Biomineralization: Perspectives on Uptake, Transport, and Deposition of Calcium, Carbonate, and Phosphate** *J. Am. Chem. Soc* **143** <https://doi.org/10.1021/jacs.1c09174>
- Kutschera U, Briggs WR (2016) **Phototropic solar tracking in sunflower plants: an integrative perspective** *Annals of Botany* **117**:1–8 <https://doi.org/10.1093/aob/mcv141>
- Lee JJ (2006) **Algal symbiosis in larger foraminifera** *Symbiosis* **42**:63–75 <https://doi.org/10.1017/S2475262200002355>
- Macías-Sánchez E, Willinger MG, Pina CM, Checa AG (2011) **Transformation of ACC into aragonite and the origin of the nanogranular structure of nacre** *Scientific Reports* **7**

Matt A-S, Chang WW, Hu MY (2022) **Extracellular carbonic anhydrase activity promotes a carbon concentration mechanism in metazoan calcifying cells** *PNAS* **119** <https://doi.org/10.1073/pnas.2203904119>

Meldrum FC, Cölfen H (2008) **Controlling mineral morphologies and structures in biological and synthetic systems** *Chemical Reviews* **108**:4332–4432 <https://doi.org/10.1021/cr8002856>

Mordhorst T, Awal S, Jordan S, Petters C, Sartoris L, Dringen R, Bickmeyer U (2015) **The chemically synthesized ageladine A-derivative LysoGlow84 stains lysosomes in viable mammalian brain cells and specific structures in the marine flatworm *Macrostomum lignano*** *Marine Drugs* **13**:920–935 <https://doi.org/10.3390/md13020920>

Nagai Y, Tsubaki R, Fujita K, Toyofuku T (2023) **Ultrafine structure observation and pH imaging of site of calcification in *Sorites orbiculus*** *International Symposium on Foraminifera, Peruggia, FORAMS 2023 Grzybowski Foundation Special Publication No 27*

de Nooijer LJ, Toyofuku T, Kitazato H (2009) **Foraminifera promote calcification by elevating their intracellular pH** *Proc. Natl. Acad. Sci. USA* **106**:15374–15378 <https://doi.org/10.1073/pnas.0904306106>

de Nooijer LJ, Toyofuku T, Oguri K, Nomaki H, Kitazato H (2008) **Intracellular pH distribution in foraminifera determined by the fluorescent probe HPTS** *Limnology and Oceanography: Methods* **6**:610–618

Parker JH (2017) **Ultrastructure of the test wall in modern porcelaneous foraminifera: implications for the classification of the Miliolida** *Journal of Foraminiferal Research* **47**:136–174

Pawlowski J, Holzmann M, Tyszka J (2013) **New supraordinal classification of Foraminifera: Molecules meet morphology** *Marine Micropaleontology* **100**:1–10

Prazeres M., Renema W (2019) **Evolutionary significance of the microbial assemblages of large benthic Foraminifera** *Biological Reviews* **94**:828–848

Raz S, Weiner S, Addadi L (2000) **Formation of high-magnesian calcites via an amorphous precursor phase: possible biological implications** *Advanced Materials* **12**:38–42 [https://doi.org/10.1002/\(SICI\)1521-4095\(200001\)12:1<38::AID-ADMA38>3.0.CO;2-I](https://doi.org/10.1002/(SICI)1521-4095(200001)12:1<38::AID-ADMA38>3.0.CO;2-I)

Raz S, Hamilton PC, Wilt FH, Weiner S, Addadi L (2003) **The transient phase of amorphous calcium carbonate in sea urchin larval spicules: the involvement of proteins and magnesium ions in its formation and stabilization** *Advanced Functional Materials* **13**:480–486

Seto J *et al.* (2012) **Structure-property relationships of a biological mesocrystal in the adult sea urchin spine** *Proc. Natl. Acad. Sci. USA* **9**:3699–3704

Sturm EV, Cölfen H (2016) **Mesocrystals: structural and morphogenetic aspects** *Chem Soc. Rev* **45**

Sturm EV, Cölfen H (2017) **Mesocrystals: Past, Presence** *Crystals* **7**

Sviben S *et al.* (2016) **A vacuole-like compartment concentrates a disordered calcium phase in a key coccolithophorid alga** *Nature Communication* **7**:1–9

- Towe KM, Cifelli R (1967) **Wall ultrastructure in the calcareous foraminifera: crystallographic aspects and a model for calcification** *Journal of Paleontology* **41**:742–762
- Toyofuku T., Matsuo M., de Nooijer L., et al. (2017) **Proton pumping accompanies calcification in foraminifera** *Nature Communication* **8** <https://doi.org/10.1038/ncomms14145>
- Tyszka T, Bickmeyer U, Raitzsch M, Bijma J, Kaczmarek K, Mewes A, Topa P, Janse M (2019) **Form and function of F-actin during biomineralization revealed from live experiments on foraminifera** *Proc. Natl. Acad. Sci. USA* **116**:4111–4116
- Tyszka J, Godos K, Goleń J, Radmacher W (2021) **Foraminiferal organic linings: Functional and phylogenetic challenges** *Earth-Science Reviews* **220**
- de Vrind-de Jong EW, Borman A, Thierry P, Westbroek P, Gruter M, Kamerling JP (1986) **Calcification in the coccolithophorids *Emiliana huxleyi* and *Pleurochrysis carterae* II. Biochemical aspects. B.S.C. Leadbeater** *Biomineralization in Lower Plants and Animals* :205–217
- Weiner S, Addadi L (2011) **Crystallization pathways in biomineralization** *Annual Review of Materials Research* **41**:21–40 <https://doi.org/10.1146/annurev-matsci-062910-095803>
- Weiner S, Levi-Kalisman Y, Raz S, Addadi L (2003) **Biologically formed amorphous calcium carbonate** *Connective Tissue Research* **44**:214–218
- Weiss MI, Tuross N, Addadi L, Weiner S (2002) **Mollusc larval shell formation: amorphous calcium carbonate is a precursor phase for aragonite** *Journal of Experimental Zoology* **293**:478–491

## Editors

Reviewing Editor

**Meike Stumpp**

Christian-Albrechts University of Kiel, Kiel, Germany

Senior Editor

**Claude Desplan**

New York University, New York, United States of America

## Reviewer #1 (Public Review):

Summary:

The manuscript by Dubicka and co-workers on calcification in miliolid foraminifera presents an interesting piece of work. The study uses confocal and electron microscopy to show that the traditional picture of calcification in porcelaneous foraminifera is incorrect.

Strengths:

The authors present high-quality images and an original approach to a relatively solid (so I thought) model of calcification.

Weaknesses:

There are several major shortcomings. Despite the interesting subject and the wonderful images, the conclusions of this manuscript are simply not supported at all by the results. The

fluorescent images may not have any relation to the process of calcification and should therefore not be part of this manuscript. The SEM images, however, do point to an outdated idea of miliolid calcification. I think the manuscript would be much stronger with the focus on the SEM images and with the speculation of the physiological processes greatly reduced.

Comments on revised version:

I continue to disagree. As the authors acknowledge: 'may be a hint indicating ACC...', but it may also be something else. This is really something else than showing ACC is involved in foraminiferal calcification. I still think the reasoning is shaky and below, I will clarify why the fluorescence may well not be related to ACC and in fact, some or even most of the vesicles may not play the role that the authors suggest. Even if they do, the conclusions are not supported by the data presented here. Unfortunately, I found some of the other answers to my question not satisfactory either.

<https://doi.org/10.7554/eLife.91568.2.sa2>

### **Reviewer #2 (Public Review):**

Summary:

Dubicka et al. in their paper entitled "Biocalcification in porcelaneous foraminifera" suggest that in contrast to the traditionally claimed two different modes of test calcification by rotallid and porcelaneous miliolid foraminifera, both groups produce calcareous tests via the intravesicular mineral precursors (Mg-rich amorphous calcium carbonate). These precursors are proposed to be supplied by endocytosed seawater and deposited in situ as mesocrystals formed at the site of new wall formation within the organic matrix. The authors did not observe the calcification of the needles within the transported vesicles, which challenges the previous model of miliolid mineralization. Although the authors argue that these two groups of foraminifera utilize the same calcification mechanism, they also suggest that these calcification pathways evolved independently in the Paleozoic.

Comments on the revised version

In my reply to the author's rebuttal letter, I will focus on one key point. The main observation supporting the author's conclusion, as expressed in the abstract, is:

"We found that both groups [i.e., rotaliids and miliolids, the latter documented in the reviewed paper] produced calcareous shells via the intravesicular formation of unstable mineral precursors (Mg-rich amorphous calcium carbonates) supplied by endocytosed seawater and deposited at the site of new wall formation within the organic matrix. Precipitation of high-Mg calcitic mesocrystals took place in situ and formed a dense, chaotic meshwork of needle-like crystallites."

In my review, I pointed out that there is no support for the existence of an intracellular, vesicular intermediate amorphous phase.

The authors replied:

"We used laser line 405 nm and multiphoton excitation to detect ACCs. These wavelengths (partly) permeate the shell to excite ACCs autofluorescence. The autofluorescence of the shells is present as well but not clearly visible in movie S4 as the fluorescence of ACCs is stronger. This may be related to the plane/section of the cell which is shown. The laser permeates the shell above the ACCs (short distance) but to excite the shell CaCO<sub>3</sub> around foraminifera in the same three-dimensional section where ACCs are shown, the light must pass a thick CaCO<sub>3</sub> area due to the three-dimensional structure of the foraminiferan shell. Therefore, the laser



light intensity is reduced. In a revised version, a movie/image with reduced threshold is shown."

This reply does not address the reviewer's concerns. Detection of ACC with 405 nm excitation is not sufficient; many organic components can fluoresce under violet light excitation. For example, Delvene et al. (2002) (<https://doi.org/10.18261/let.55.4.7>) showed that "the Pleistocene and Jurassic microborings emit in the blue-yellow spectral region (420-600 nm) with a laser excitation of 405 nm, which coincides with the emission due to NADPH [nicotinamide adenine dinucleotide], FAD [flavin adenine dinucleotide], and riboflavin pigments characteristic of some cyanobacteria." Traditionally, in geological or biogenic calcium carbonate samples, Raman spectroscopic characterization of ACC and its magnesium content can be used (e.g., Wang, D., Hamm, L. M., Bodnar, R. J. & Dove, P. M. Raman spectroscopic characterization of the magnesium content in amorphous calcium carbonates. *J. Raman Spectrosc.* 43, 543-548 (2012); Perrin, J. et al. Raman characterization of synthetic magnesian calcites. *Am. Mineral.* 101, 2525-2538 (2016)). However, in biological, living-cell systems, Mehta et al. (2022) (doi: 10.1016/j.saa.2022.121262) successfully used FTIR spectroscopy to identify ACC by two characteristic FTIR vibrations at ca. 860 cm<sup>-1</sup> and ca. 306 cm<sup>-1</sup>. Other methods such as STXM analyses at the C K-edge (Monteil et al. 2021, doi: 10.1038/s41396-020-00747-3) are also available. Because the core of the authors' interpretation (i.e., detection of ACC in vesicles) is not supported by hard evidence, the claim that the study represents a "paradigm shift" is far-fetched and the whole model is based on speculations. If the authors are able to unequivocally confirm the presence of ACC within the vesicles and its subsequent transformation into calcitic needles, the other problems noted in the paper will be relatively trivial.

<https://doi.org/10.7554/eLife.91568.2.sa1>

#### Author response:

The following is the authors' response to the original reviews.

##### **Reviewer #1 (Public Review):**

###### *Summary:*

*The manuscript by Dubicka and co-workers on calcification in miliolid foraminifera presents an interesting piece of work. The study uses confocal and electron microscopy to show that the traditional picture of calcification in porcelaneous foraminifera is incorrect.*

###### *Strengths:*

*The authors present high-quality images and an original approach to a relatively solid (so I thought) model of calcification.*

###### *Weaknesses:*

*There are several major shortcomings. Despite the interesting subject and the wonderful images, the conclusions of this manuscript are simply not supported at all by the results. The fluorescent images may not have any relation to the process of calcification and should therefore not be part of this manuscript. The SEM images, however, do point to an outdated idea of miliolid calcification. I think the manuscript would be much stronger with the focus on the SEM images and with the speculation of the physiological processes greatly reduced.*

We agree that fluorescence studies presented in the paper are not an unequivocal proof by itself for calcification model utilised by studied Miliolida species. However, fluorescence data combined with SEM studies, especially overlap of the elements that show autofluorescence upon excitation at 405 nm (emission 420–480 nm) and acidic vesicles marked by p\_H-sensitive LysoGlow84, may be a hint indicating ACC-bearing vesicles.

We will tone down the the physiological interpretation based on fluorescence studies in the revised version of the manuscript.

Nevertheless, we think that our fluorescent life-imaging experiments provides important observations in miliolida, which is scarce in the existing literature, and therefore are worth being presented as they might be very helpful in better understanding of full calcification model in the future.

**Reviewer #2 (Public Review):**

*Summary:*

*Dubicka et al. in their paper entitled "Biocalcification in porcelaneous foraminifera" suggest that in contrast to the traditionally claimed two different modes of test calcification by rotallid and porcelaneous miliolid foraminifera, both groups produce calcareous tests via the intravesicular mineral precursors (Mg-rich amorphous calcium carbonate). These precursors are proposed to be supplied by endocytosed seawater and deposited in situ as mesocrystals formed at the site of new wall formation within the organic matrix. The authors did not observe the calcification of the needles within the transported vesicles, which challenges the previous model of miliolid mineralization. Although the authors argue that these two groups of foraminifera utilize the same calcification mechanism, they also suggest that these calcification pathways evolved independently in the Paleozoic.*

We do not argue that Miliolida and Rotallida utilize exactly the same calcification mechanism but the both groups use less divergent crystallization pathways, where mesocrystalline chamber walls are created by accumulating and assembling particles of pre-formed liquid amorphous mineral phase.

*Strengths:*

*The authors document various unknown aspects of calcification of Pseudolachlanella eburnea and elucidate some poorly explained phenomena (e.g., translucent properties of the freshly formed test) however there are several problematic observations/interpretations which in my opinion should be carefully addressed.*

*Weaknesses:*

*(1) The authors (line 122) suggest that "characteristic autofluorescence indicates the carbonate content of the vesicles (Fig. S2), which are considered to be Mg-ACCs (amorphous MgCaCO<sub>3</sub>) (Fig. 2, Movies S4 and S5)". Figure S2 which the authors refer to shows only broken sections of organic sheath at different stages of mineralization. Movie S4 shows that only in a few regions some vesicles exhibit red autofluorescence interpreted as Mg-ACC (S5 is missing but probably the authors were referring to S3). In their previous paper (Dubicka et al 2023: Heliyon), the authors used exactly the same methodology to suggest that these are intracellularly formed Mg-rich amorphous calcium carbonate particles that transform into a stable mineral phase in rotaliid Aphistegina lessonii. However, in Figure 1D (Dubicka et al 2023) the apparently carbonate-loaded vesicles show the same red autofluorescence as the test, whereas in their current paper, no evidence of autofluorescence of Mg-ACC grains accumulated*

*within the "gel-like" organic matrix is given. The S3 and S4 movies show circulation of various fluorescing components, but no initial phase of test formation is observable (numerous mineral grains embedded within the organic matrix - Figures 3A and B - should be clearly observed also as autofluorescence of the whole layer). Thus the crucial argument supporting the calcification model (Figure 5) is missing.*

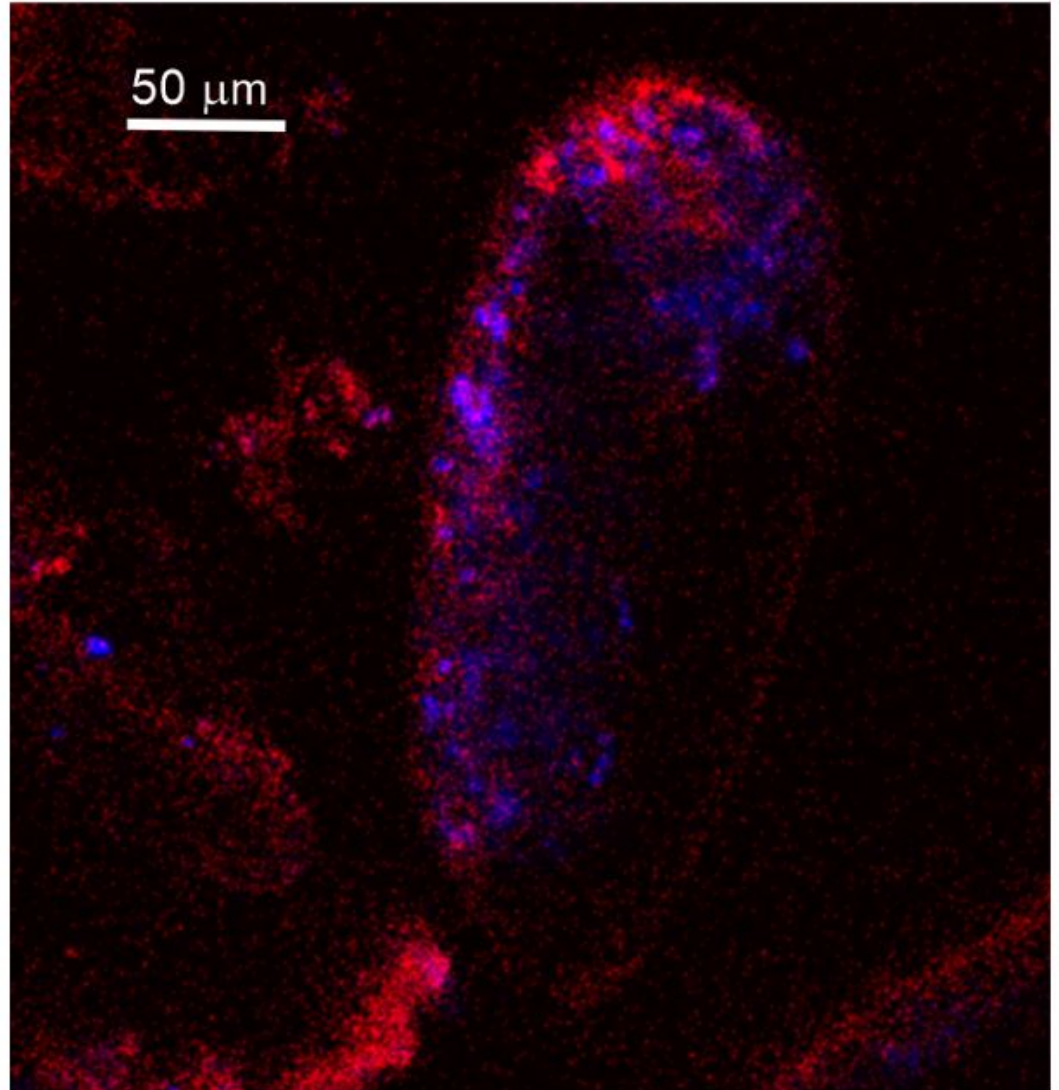
This is correct that we did not observe the initial phase of test formation *in vivo*. Therefore, it is not our crucial argument supporting novel components of the new calcification model. We suspect that vesicles preparing and transporting Mg-ACC are produced way before their docking and deposition into the new wall, because such seawater vesicles were observed between the chamber formation stages (Goleń and Tyszka, 2024, personal communication based on independent experiments on a closely related miliolid taxon). It means that our *in vivo* experiments most likely represent a long, dynamic stage of vesicles formation via seawater endocytosis, their modification (incl. Mg-ACC formation) before the stage of exocytosis during the new chamber formation. Our crucial arguments supporting the calcification model come from the SEM imaging of the specimens fixed during chamber formation, as well as from the transparency of the new chamber wall during its progressive calcification.

*There is no support for the following interpretation (lines 199-203) "The existence of intracellular, vesicular intermediate amorphous phase (Mg-ACC pools), which supply successive doses of carbonate material to shell production, was supported by autofluorescence (excitation at 405 nm; Fig. 2; Movies S3 and S4; see Dubicka et al., 2023) and a high content of Ca and Mg quantified from the area of cytoplasm by SEM-EDS analysis (Fig. S6)."*

We used laser line 405nm and multiphoton excitaton to detect ACCs. These wavelengths (partly) permeate the shell to excite ACCs autofluorescence. The autofluorescence of the shells is present as well but not clearly visible in movieS4 as the fluorescence of ACCs is stronger. This may be related to the plane/section of the cell which is shown. The laser permeates the shell above the ACCs (short distance) but to excite the shell CaCO<sub>3</sub> around foraminifera in the same three-dimensional section where ACCs are shown, the light must pass a thick CaCO<sub>3</sub> area due to the three-dimensional structure of the foraminiferan shell. Therefore, the laser light intensity is reduced. In a revised version a movie/image with reduced threshold is shown.

#### **Author response image 1.**

Autofluorescence image of studied Miliolida species (exc. 405 nm) showing algal chlorophyll (blue) and CaCO<sub>3</sub> (red), both ACC and calcite shell.



*It would be very convenient if it was possible to visualize ACC by illumination with a blacklight, but there are very many organic molecules that have an autofluorescence excited by ~405 nm. One of the examples is NADH (Lee et al., 2015. Kor J Physiol Pharmac 19(4): 373-382), an omnipresent molecule in any cell (couldn't copy the appropriate picture here, but the reference has a figure with the em/exc spectra).*

The paper of Lee et al. 2015 shows that the excitation spectrum of NADH is ending close to 400 nm. This means that NADH is not or only very weakly excitable at 405nm, what we used as the excitation laser line.

*(2) The authors suggest that "no organic matter was detected between the needles of the porcelain structures (Figures 3E; 3E; S4C, and S5A)". Such a suggestion, which is highly unusual considering that biogenic minerals almost by definition contain various organic components, was made based only on FE-SEM observation. The authors should either provide clearcut evidence of the lack of organic matter (unlikely) or may suggest that intense calcium carbonate precipitation within organic matrix gel ultimately results in a decrease of the amount of the organic phase (but not its complete elimination), alike the pure calcium carbonate crystals are separated from the remaining liquid with impurities*



*("mother liquor"). On the other hand, if (249-250) "organic matrix involved in the biomineralization of foraminiferal shells may contain collagen-like networks", such "laminar" organization of the organic matrix may partly explain the arrangement of carbonate fibers parallel to the surface as observed in Fig. 3E1.*

We agree with the reviewer that biogenic minerals should by definition contain some organic components. We just wrote that "no organic matter was detected between the needles of the porcelain structures" that means that we did not detect any organic structures based only on our FE-SEM observations. We will rephrase this part of the text to avoid further confusion.

*(3) The author's observations indeed do not show the formation of individual skeletal crystallites within intracellular vesicles, however, do not explain either what is the structure of individual skeletal crystallites and how they are formed. Especially, what are the structures observed in polarized light (and interpreted as calcite crystallites) by De Nooijer et al. 2009? The author's explanation of the process (lines 213-216) is not particularly convincing "we suspect that the OM was removed from the test wall and recycled by the cell itself".*

Thank you for this comment. We will do our best to supplement our explanations. We are aware about the structures observed in polarized light by De Nooijer et al. (2009). However, Goleń et al. (2022, Prostist; + 2 other citations) showed that organic polymers may also exhibit light polarization. Additional experimental studies are needed to separate these types of polarization. We will try to investigate this issue in our future research.

*(4) The following passage (lines 296-304) which deals with the concept of mesocrystals is not supported by the authors' methodology or observations. The authors state that miliolid needles "assembled with calcite nanoparticles, are unique examples of biogenic mesocrystals (see Cölfen and Antonietti, 2005), forming distinct geometric shapes limited by planar crystalline faces" (later in the same passage the authors say that "mesocrystals are common biogenic components in the skeletons of marine organisms" (are they thus unique or are they common)? It is my suggestion to completely eliminate this concept here until various crystallographic details of the miliolid test formation are well documented.*

Our intension was to express that mesocrystals are common biogenic components in the skeletons of marine organisms however such a miliolid needles forming distinct geometric shapes limited by planar crystalline faces are unique.

**Reviewer #1 (Recommendations For The Authors):**

*Below, I have summarized my main criticisms.*

*(1) The movies S1-S4 do not indicate what is described. The videos show indeed seawater (S1), cell membranes (S2), and autofluorescence and acidic vesicles (S3 and S4). The presence of all these intracellular structures is not surprising: any eukaryotic cell will have those. The authors, however, claim that they participate in the process of calcification, which is simply not shown. One of the main arguments seems the presence of 'carbonate pools', in the caption these are even claimed to be 'Mg-ACC pools', but this is by no means revealed by an excitation of 405nm/ emission between 420 and 490 nm. It would be very convenient if it was possible to visualize ACC by illumination with a blacklight, but there are very many organic molecules that have an autofluorescence excited by ~405 nm. One of the examples is NADH (Lee et al., 2015. Kor J Physiol Pharmac 19(4): 373-382), an omnipresent molecule in any cell (couldn't copy the appropriate picture here, but the reference has a figure with the em/exc spectra).*

The paper of Lee et al. 2015 shows that the excitation spectrum of NADH is ending close to 400 nm. This means that NADH is not or only very weakly excitable at 405nm, what we used as the excitation laser line.

*The fluorescence by this excitation/ emission couple unlikely indicates the vesicles in which these foraminifera calcify. Therefore, most of the interpretation of the authors on what happens with the calcitic needles is not based on results but remains pure speculation.*

The fluorescence autofluorescence upon excitation at 405 nm (emission 420–480 nm is typical for CaCO<sub>3</sub> both for biocalcite and amorphous calcium carbonate, what was proven by laboratory synthesis of amorphous calcium carbonate (Dubicka et al., in preparation).

*(2) The results mention 'granules', which are the supposed Mg-ACC-containing vesicles, but the movies simply don't show any granules. Only fluorescence. Again, the results show a lot of vesicles with autofluorescence, but these are not necessarily related to calcification. Proof could be supplied by showing that the same fluorescent vesicles are 'used up' when the specimens under observation are making a new chamber, but until that is done, the fate of all these vesicles remains uncertain and once more, may not be involved in calcification at all.*

We suspect that vesicles preparing and transporting Mg-ACC are produced way before their docking and deposition into the new wall, because such seawater vesicles were observed between the chamber formation stages (Goleń and Tyszka, 2024, personal communication based on independent experiments on a closely related miliolid taxon). It means that our *in vivo* experiments most likely represent a long, dynamic stage of vesicles formation via seawater endocytosis, their modification (incl. Mg-ACC formation) before the stage of exocytosis during the new chamber formation. Our crucial arguments supporting the calcification model come from the SEM imaging of the specimens fixed during chamber formation, as well as from the transparency of the new chamber wall during its progressive calcification.

*(3) The Methods are unclear. How long were the foraminifers kept before being placed under the microscope? Were they fed with anything? This is important since the chlorophyll should not be from any food source. I didn't know that this foraminiferal species has photosynthetic symbionts: genera like *Quinqueloculina* don't. Is there any reference for this? Normally, I wouldn't care that much, but the authors find the presence of (facultative) symbionts important (lines 305-336). I am a bit suspicious about this since the only evidence for the presence of photosynthetic symbionts is because of the autofluorescence. As the authors said, commonly these miliolid species are regarded as symbiont-barren, so additional proof for these symbionts is necessary.*

We agree that additional proof is needed for the presence of photosynthetic symbionts. We rephrased the manuscript accordingly.

*(4) It is also unclear (Methods) at what stage the miliolids were photographed (Figure 3). How did chamber formation proceed, what was the timing of the photographs, etc. These pictures are to me the most interesting finding of this study, but need to be described much better.*

All individuals of living foraminifera were fixed at the overall stage of chamber formation. However, every individual presents a complete set of successive steps (substages) of chamber wall calcification fixed at once. Fig. 3A and B present nearly the most proximal (youngest)

part of the new chamber with a thick wall of calcite nanograins within a gel-like organic matrix. Fig. 3C and D present a bit more distal (intermediate) part of the calcified chamber. Fig. 3E shows the most distal part of the new chamber. This part is anchored to the older, underlying solid calcified chamber (not shown in this figure). All these steps are synchronous, however, represent gradual successive stages of calcification. The main text and Figs 4 and 5 explain this phenomenon in details.

*There are many small issues with the text too. These include:*

*Line 28/29: in many other groups, calcification is thought to be polyphyletic (e.g. sponges: Chombard et al., 1997. Biol Bull 193: 359-367).*

Corrected

*Line 29/30: there may be even more 'types of shells'. The first author has shown in earlier papers that nodosarids have a unique shell architecture. Spirillinids also seem to have their own way of calcification. It is unclear what is meant here by 'two contrasting models'.*

By now there are known only two models of foraminiferal calcification. Lagenida biocalcification has not been studied.

*Line 33: 'Both groups'? This paper only shows calcification in miliolids.*

However, we refer to previous study.

*Line 42: Perhaps, but there is no data on the pseudopodial network in this manuscript.*

We refer to Angell, 1980 studies

*Line 43: Likely, but that is not what this manuscript is showing.*

*Line 42-44: The authors should make a choice and be clear. The point of this paper is that miliolids and rotalids calcify in ways that are actually not as different as they seemed previously. Still, they are said to have different 'chamber formation modes'. If they are calcifying in a similar way (which I think is not necessarily supported by the results), isn't calcification in these groups like variations on the same theme? How does this relate to the independent origins of calcification within these two groups?*

Our intension is to show that Miliolida and Rotaliida utilize less divergent calcification pathways, following the recently discovered biomineralization principles.

*Line 49-51: is this a well-established distinction? If so, please add a reference. If not: what is fundamentally different between B and C? Does only the size of the intracellular vesicle matter?*

Rephrased

*Line 60: please include a reference for the intracellular calcification by coccolithophores.*

Added

*Line 67: this is wrong. It is the alignment of the needles at the surface that makes them all reflect light in the same way and gives the shells a porcelaneous appearance. A close-*

*up of the miliolid's shell surface shows this arrangement. Underneath this layer, the orientation of the needles is more random.*

We referred to Johan Hohenegger papers.

*Line 114: how else?*

*Line 114-116: I don't see the relevance here. If seawater is taken up, the vesicle containing this seawater has to have a membrane around it. By definition. The text here ('These vesicles') suggests that Calcein and FM1-43 were combined (which they easily could have), but the methods describe that they are used successively.*

Yes, we used two dyes separately.

*Lines 122-130: I think the interpretation of this autofluorescence signal is wrong. Even if it was true, these lines belong to the Discussion.*

This paragraph has been placed within discussion

*Line 138: What are 'mobile clusters'? I don't see a relation between the location of the symbionts and the other vesicles (Figure 2).*

*Line 147-148: How can an SEM image show the absence of organic matter?*

We meant the absence of the gel-like OM visible in the previous stages of the chamber formation

*Line 148: Should be 'Figs. 3E; 3E1; S4C'.*

Corrected

*Lines 143-150: this can be merged with the following paragraph.*

Done

*Lines 151-169: why is there no indication of the time? Figures 3 and 4 link the pictures in time to show the development of the growing chamber wall. However, neither here nor in the methods, is there any recording of the time after the beginning of chamber formation. Now, the images are linked (Figure 4) as if they were taken at regular intervals, but this is not documented.*

*Lines 170-184: this should go to the Discussion.*

Done

*Line 193-195: this is likely, but not visible in Figure 1.*

It was visible by optical microscopy and described by Angell, 1980

*Line 199-201: I don't understand this: the fluorescent vesicles were not observed during chamber formation so any link between the SEM and CLSM scans remains pure speculation.*

*Line 203-204: needed for what?*

For better documentation of Miliolid ACC-bearing granules

| *Line 220: is this shown in any of the images?*

Angell, 1980

| *Line 230: It sounds nice, but I don't think a 'paradigm shift' is appropriate here. However interesting and important foraminiferal biomineralization is, the authors show that the crystals of miliolids are likely formed differently than previously thought. If this is a 'paradigm shift', then most scientific findings are.*

In our opinion this is definitely a shift of paradigm

| *Line 231: I don't think anyone suggested miliolids and coccolithophores share 'the same' pathway. They are shown (cocco's) and thought (miliolids) to secrete their calcite intracellularly.*

Changed to similar, intracellular

| *Line 258: References should only be to peer-reviewed studies.*

| *Line 430: Burgers'*

Corrected

| **Reviewer #2 (Recommendations For The Authors):**

| *Please separate clearly the results (observations) from the discussion (interpretations): various interpretational/commentary phrases should be removed from the Results section to Discussion e.g., lines 124-130, 131-135.*

Interpretation have been separated from results as suggested by Reviewer.

| *[line 49] "living cells have evolved three major skeleton crystallization pathways". I would rather say "organisms" not "cells" as the coordination of the calcification process in multicellular organisms clearly involves processes that are beyond the individual cell activity.*

Corrected

<https://doi.org/10.7554/eLife.91568.2.sa0>